LEAPT: Lectin-directed enzyme-activated prodrug therapy

Mark A. Robinson*, Stuart T. Charlton†, Philippe Garnier*, Xiang-tao Wang*, Stanley S. Davis†, Alan C. Perkins‡, Malcolm Frier‡, Ruth Duncan§, Tony J. Savage¶, David A. Wyatt¶, Susan A. Watson‖, and Benjamin G. Davis*,**

*Chemistry Research Laboratory, Department of Chemistry, University of Oxford, Mansfield Road, Oxford OX1 3TA, United Kingdom; †Institute of Pharmaceutical Sciences, University of Nottingham, University Park, Nottingham NG7 2RD, United Kingdom; ‡Department of Medical Physics, Medical School, Queen's Medical Centre, Nottingham NG7 2UH, United Kingdom; §Welsh School of Pharmacy, King Edward VII Avenue, Cardiff University, Cardiff CF10 3XF, United Kingdom; ¶GlaxoSmithKline, Medicines Research Centre, Gunnels Wood Road, Stevenage SG1 2NY, United Kingdom; and ‖Academic Unit of Cancer Studies, University of Nottingham, Queen's Medical Centre, Nottingham NG7 2UH, United Kingdom

Targeted drug delivery to selected sites allows reduced toxicity, enhanced efficiency and interchangeable target potential [Langer, R. (2001) *Science* 293, 58–59 and Molema, G. & Meijer, D. K. F., eds. (2001) *Drug Targeting* (Wiley-VCH, Weinheim, Germany)]. We describe a bipartite drug-delivery system that exploits (*i*) endogenous carbohydrate-to-lectin binding to localize glycosylated enzyme conjugates to specific, predetermined cell types followed by (*ii*) administration of a prodrug activated by that predelivered enzyme at the desired site. The carbohydrate structure of an α-L-rhamnopyranosidase enzyme was specifically engineered through enzymatic deglycosylation and chemical reglycosylation. Combined *in vivo* and *in vitro* techniques (gamma scintigraphy, microautoradiography and confocal microscopy) determined organ and cellular localization and demonstrated successful activation of α-L-rhamnopyranoside prodrug. Ligand competition experiments revealed enhanced, specific localization by endocytosis and a strongly carbohydrate-dependent, 60-fold increase in selectivity toward target cell hepatocytes that generated a >30-fold increase (from 0.02 to 0.66 mg) in protein delivered. Furthermore, glycosylation engineering enhanced the serum-uptake rate and enzyme stability. This created enzyme activity (0.2 units in hepatocytes) for prodrug therapy, the target of which was switched simply by sugar-type alteration. The therapeutic effectiveness of lectin-directed enzyme-activated prodrug therapy was shown through the construction of the prodrug of doxorubicin, Rha-DOX, and its application to reduce tumor burden in a hepatocellular carcinoma (HepG2) disease model.

Carbohydrates are often key ligands in nature (1), and many specific carbohydrate-based ligand–receptor mechanisms have been implicated in processes such as inflammation (2), cell surface communication (3), and immune response (1). Carbohydrates exhibit properties of potential interest when developing drug-delivery mechanisms, such as specificity in their interaction with their receptors (4) and the varied nature of potentially targetable receptors available (5). Macromolecular glycoconjugates, in particular, have shown some promise (6). Synthetic glycopolymers†† and glycoproteins (7, 8) have been used as carriers of covalently conjugated drugs, bearing carbohydrate ligands that provide delivery specificity. However, these systems commonly rely on endogenous mechanisms, such as lysosomal degradation, for release of the active drug, and so the unwanted release of the drug at sites other than the desired site of action is possible. Moreover, the maximum potential loading of drug onto each macromolecule is limited and this may demand an increase in the amount of conjugate to be delivered, posing problems of dose regime and cost. As a solution to these challenges, we have investigated the potential of a catalytic system. Lectin-directed enzyme-activated prodrug therapy (LEAPT) is designed to exploit endogenous carbohydrate-lectin binding by combining it with biocatalysis through the construction of novel glycosylated enzymes and prodrugs.

Bipartite systems using biocatalysts for site-selective drug delivery have been developed by others with significant success. Antibody-directed enzyme prodrug therapy (ADEPT) (9) uses mAb–enzyme conjugates to release a prodrug at a site determined by the mAb–antigen interaction. Analogously, antibody-directed "abzyme" prodrug therapy (ADAPT) (10), where a catalytic antibody replaces the enzyme used in ADEPT, has also been investigated. In both strategies, the biocatalyst component is localized at an antigen-presenting site, typically resulting in a serum-exposed biocatalyst source. After administration of the appropriate prodrug, the active drug molecule is released by this localized enzyme, resulting in a potential reduction in selectivity due to the diffusion and uptake of active drug into nontargeted bystander cells. An additional strategy, gene-directed enzyme prodrug therapy (GDEPT) (11), involves the delivery of a gene encoding for a foreign enzyme to a chosen site, and, after subsequent enzyme expression, a dose of prodrug results in the selective release of the parent drug. GDEPT provides a source of enzyme localized within a cell, therefore reducing the problem of reduced selectivity associated with the bystander effect, but it requires the development of gene-delivery vehicles appropriate to a particular cell type.

The strategies above may require the generation of a novel selectivity between biocatalyst component and target cell. However, several highly specific and potent binding mechanisms are already present in nature and may be exploited in drug delivery (12). Among these mechanisms, the interaction of carbohydrate-binding protein lectins with carbohydrates is one of potential utility (2) that has been particularly highlighted by serum-clearance studies of glycoproteins by the asialoglycoprotein receptor (ASGPR) (13) and the mannose receptor (14). The ASGPR protein is a membrane-bound, endocytic lectin found in abundance on the surface of hepatocytes in the liver (15). The ASGPR was first exploited in carbohydrate-mediated macromolecular drug delivery in 1983 (16), but various examples have since been demonstrated (6). The targeting of enzymes by carbohydrate receptors has been demonstrated, but only when that enzyme itself is the therapeutic agent (17–20). To exploit such natural carbohydrate-binding mechanisms, the LEAPT approach uses two components: the cell-specific delivery of a synthetically glycosylated enzyme, here an α-rhamnosidase, and an appropriately capped, here rhamnoside-capped, prodrug (Fig. 1*A*). The glycosylated α-rhamnosidase se-
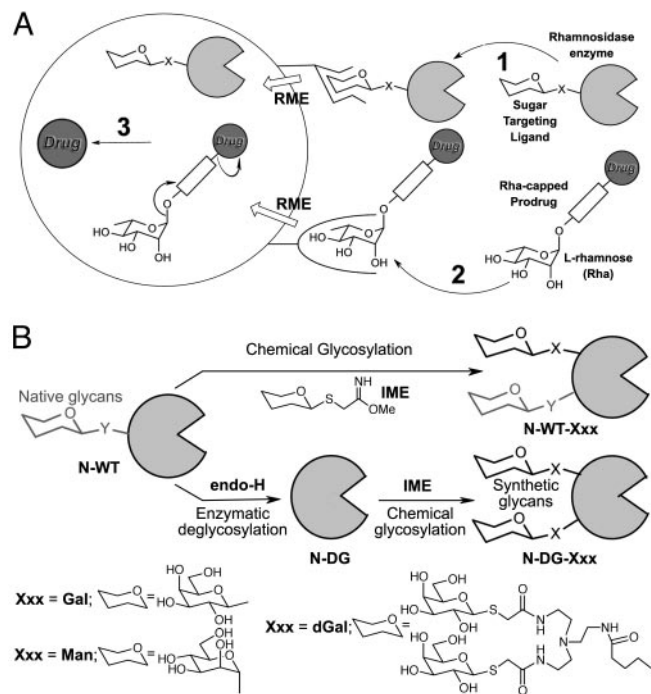
PHARMACOLOGY

Fig. 1. The LEAPT strategy. (*A*) Concept. LEAPT is a bipartite delivery system. (Step 1) Site-selective delivery of a glycosylated rhamnosidase (Rha-cleaving) enzyme by sugar-mediated RME. (Step 2) Delivery of a Rha-capped prodrug that can be cleaved only by the delivered glycosylated rhamnosidase. When these two steps are combined, activation of the prodrug results in site-selective release of the parent drug (Step 3). (*B*) Glycosylated enzyme construction. Pure wild-type α-L-rhamnosidase N-WT with native ''Y-linked'' glycosylation was (*i*) chemically glycosylated with sugar-IME reagents to yield a N-WT-Xxx (Xxx = Gal, Man, or dGal) series with mixed synthetic (''X-linked'') and native (Y-linked) glycosylation or (*ii*) enzymatically DG with endo-H, yielding N-DG. N-DG was then chemically reglycosylated with sugar-IME reagents to yield only synthetic (X-linked) N-DG-Xxx (15). An IME reagent bearing two terminal Gal units (dGal) was also synthesized from D-galactose.

lected here, a nonmammalian glycosidase enzyme, is delivered to specific cell types within the body and mediated by preselected carbohydrate–receptor interactions as determined by appropriate choice of carbohydrate. Once uptake is complete, a prodrug composed of a drug molecule bearing an α-L-rhamnoside cap can be dosed. As L-rhamnopyranose (Rha) is of nonmammalian origin, Rha-capped prodrugs cannot be processed by mammalian enzymes, ensuring that the parent drug is released primarily by the prelocalized α-rhamnosidase. We suggest that this strategy might exhibit potential flexibility in allowing a toolkit of drug delivery to be developed by the modular variation of the target-cell receptor, through variation of sugars on the enzyme, and the parent drug. In addition, by exploiting receptor-mediated endocytosis (RME), the nonmammalian enzyme may be rapidly cleared from circulation.

Materials and Methods

Preparation of Glycosylated Enzymes. Naringinase (N) from *Penicillium decumbens* was purified to yield N-WT by dialysis (12,000–14,000 molecular weight cutoff; 5 liters × 5), Bio-Gel P100 size-exclusion chromatography (eluant, pH 4.8/0.1 M NaCl), and DEAE-Sepharose ion-exchange chromatography (eluant, pH 6.0/20 mM L-histidine/0–0.35 mM NaCl gradient). N-WT was deglycosylated (DG) by using endoglycosidase H (endo-H, 32 units/100 mg N-WT) in pH 6.0, 0.1 M orthophosphate buffer, 37°C, purified by dialysis (50,000 molecular weight cutoff) to give N-DG.

Proteins were glycosylated with the 2-imino-2-methoxyethyl 1-thioglycoside (IME) method (20, 21). (See supporting informa-

tion, which is published on the PNAS web site, for reagents, full experimental details and characterization.) Glycosylated enzymes were characterized by gel electrophoresis (10% SDS/PAGE, pH 8.8, Tris buffer; Vertical Slab Gel Kit, Atto Corporation, Tokyo) and matrix-assisted laser desorption ionization MS (PBS II, Ciphergen Biosystems, Fremont, CA; sinapinic acid matrix, 10 mg/ml, 3:2 water/acetonitrile, 0.2% trifluoroacetic acid). MS data follow: **N-WT**, 76,148; **N-WT-Gal**, 79,443 [N-WT + 3,295 ∼ +14 β-D-galactose (Gal)]; **N-DG**, 69,341; **N-DG-Gal**, 71,892 (N-DG + 2,551 ∼ +11 Gal); **N-DG-D-mannose (Man),** 72,857 (N-DG + 3,516 ∼ +15 Man); **N-DG-dGal**, 72,886 (N-DG-dGal + 3545 ∼ +10 Gal). Michaelis–Menten parameters were determined according to the initial-rates method ($[E]_0 = 3.1 \times 10^{-7}$ M, *para*-nitrophenyl α-L-rhamnopyranoside, 0.25–3.5 mM, pH 7.0, 0.1 M orthophosphate) and nonlinear regression by using GRAFIT 4.0.13 (Erithacus Software, Horley, U.K.).

Gamma Scintigraphy. Biodistribution studies were performed in male New Zealand White rabbits (Harlan, Bicester, U.K.). Hypnorm sedated animals ($n = 3$–4; average mass, 1 kg) were injected with ^{123}I-labeled enzyme (dose, 2.5 mg/kg; ≈3 MBq) solution in PBS. Where appropriate, blocker [100 mg/kg in PBS: asialofetuin (AF) for N-WT-Gal, N-WT-dGal, N-DG-Gal, and N-DG-dGal; mannosylated poly-L-lysine (PLL-Man) for N-WT-Man and N-DG-Man] was dosed 1 min before the dose of ^{123}I-labeled enzyme. Imaging was done on a Maxi Gamma Camera 406 (GE Medical Systems) at 1, 10, 30, 60, 90, and 120 min. Concurrent sampling of blood (≈1 ml) was in accordance with Laboratory Animal Science Association guidelines (22). After killing, organ radioactivity was determined by using a NaI-type PCA-P well counter.

Preparation of Radioiodinated Enzymes. The glycosylated enzymes were ^{123}I-labeled by using 1,3,4,6-tetrachloro-3α,6α-diphenylglycouril-mediated tyrosine iodination (23).

Preparation of Tritium-Labeled Enzymes (Example Protocol). A solution of N-WT (2.0 mg in 0.2 ml, pH 8.0, 0.1 M sodium tetraborate buffer) was added to a solution of *N*-succinimidyl-[2,3-3H] propionate (115 MBq, 3.48 TBq/mmol) in sodium tetraborate buffer (0.45 ml). After 2 h, the protein was purified by size-exclusion chromatography (Sephadex G25 PD10, eluant PBS).

Microautoradiography. Male Wistar rats (≈250 g, Charles River Laboratories) were anesthetized (1:1:5 Hypnorm/Hypnovel/water; dose, 0.8 ml/kg) and then injected with ^{3}H-labeled enzyme (dose, 2.5 mg/kg; ≈1.5 MBq, in 1 ml of PBS). Where appropriate, blocker (AF or PLL-Man) was dosed 1 min before dose. Animals were killed by an overdose of Euthatal, and livers and kidneys were removed. Two-millimeter sections ($n = 4$) were taken from different lobes and frozen in TissueTek OCT onto a cork disk for use in confocal microscopy analysis. Organ samples were embedded in wax, and 4-μm-thick sections were prepared and mounted. Residual wax was removed and the slides were coated with Ilford K-type nuclear emulsion, exposed, and developed ($n = 3$ grids per section), then tissue was stained with Mayer's hematoxylin solution.

Confocal Microscopy. Sections (7 μm) were mounted and submerged in buffer (500 μl of 145 mM NaCl/5 mM KCl/2 mM CaCl₂/1 mM MgCl₂/10 mM Hepes/10 mM glucose, pH 7.4). Mendiaxon-α-L-rhamnopyranoside (MEND-Rha, 2 mM, 50 μl) was added, and then fluorescence images (8-s interval, Leica TCS NT confocal microscope, ×10 Fluotar lens; argon laser, 360 nm excitation, 405 ± 40 nm emission) were rerecorded.

HPLC Analysis of Targeted MEND Levels. Liver and kidney samples ($n = 2$) from dosed and undosed animals 30 min after glycosylated enzyme treatment and 10 min after treatment with MEND-Rha prodrug (5 mg/kg) were homogenized, and the homogenate was

analyzed by HPLC [Spherisorb S5 ODS-2 RP C-18 column, 200 × 4.6 mm, mobile phase $H_2O/3\%$ $CH_3COOH:CH_3CN/3\%CH_3COOH$ (94:6) for 10 min, from 94:6 to 40:60 over 30 min, MEND at room temperature for 29 min, fluorescence detection excitation 340 nm, emission 425 nm].

Tumor Disease Model. Thirty-nine male MF1 nude mice (5–6 weeks old) were obtained. Under anesthetic, the spleen was gently exteriorized and HepG2 cells were introduced. After recovery, the mice were allocated to their respective groups: (*i*) doxorubicin (DOX)-Rha prodrug only 10 mg/kg i.v., three times weekly; (*ii*) enzyme only 2.5 mg/kg i.v., three times weekly; and (*iii*) enzyme (N-DG-Gal) then pro-drug (DOX-Rha) dosed 20 min after the enzyme preparation, i.v., three times weekly. At termination day 42, bromodeoxyuridine was administered, and mice were killed. Livers were weighed and formalin-fixed for histological quantification of total number of lesions per group and the total "tumor burden." (The sum of each animal's tumor burden was calculated from the approximate cell number multiplied by the number of lesions visible.)

See supporting information, which is published on the PNAS web site, for further details.

Results and Discussion

Glycosylated Enzyme Construction. A ready source of our selected biocatalyst enzyme α-L-rhamnosidase (naringinase, N) was purified on a gram scale to yield wild-type (WT) enzyme N-WT. This naturally sourced enzyme has an endogenous Man-rich carbohydrate motif (24), which may interfere with ligand-mediated therapeutic targeting and so was removed. N-WT was DG enzymatically to give N-DG by using the enzyme endo-H (25). This mild treatment removed $\approx$90 ($\pm$5)% of the existing carbohydrates as judged by exhaustive, destructive chemical deglycosylation with HF (26), but advantageously did not abolish catalytic activity.

We selected Gal as the cell-specific ligand to be used in synthetic, chemical enzyme glycosylation (Fig. 1B). Gal is the carbohydrate ligand preferentially bound by the 50,000–500,000 copies of the ASGPR that are typically found on a liver cell hepatocyte surface. Enhanced binding to and uptake of macromolecules by the ASGPR can be achieved by tailoring the number and, therefore, density of ligands on a given macromolecule surface (27). In particular, the interaction between carbohydrate ligand and receptor may be enhanced by the multivalent or cluster effect (28); pioneering work by Lee *et al.* (28) demonstrated a 1×10^6-fold enhancement in binding of tetraantennary over monoantennary Gal-terminated ligands to the ASGPR. This multivalent effect may be exploited in two modes: by displaying numerous copies of a monosaccharide or by the use of branched saccharides. We explored both modes by using multiple monosaccharide glycosylation (Fig. 1B, Xxx = Gal, Man) and by the development of a branched disaccharide unit, dGal (Fig. 1B, Xxx = dGal).

Among the several methods available for the construction of glycoproteins (29), chemical glycosylation offers advantages, such as precise control of sugar and ease of scale-up, and affords straightforward access to well defined glycoproteins. Lysine groups in N-WT and N-DG were chemically glycosylated by using the IME method (20, 21). Monosaccharide Gal and Man IME reagents and the branched dGal IME reagent were prepared and incubated with both N-WT and N-DG to yield a representative range of multiply monosaccharide-glycosylated enzymes (N-WT→N-WT-Gal or →N-WT-Man and N-DG→N-DG-Gal or →N-DG-Man) and readily constructed branched glycoprotein enzymes (N-WT→N-WT-dGal and N-DG→N-DG-dGal) (Fig. 1B). This combined enzymatic and chemical glycosylation engineering was achieved on gram scales and allowed the originally Man-rich carbohydrates on N-WT to be conveniently switched to DG (N-DG), Gal-rich (N-DG-Gal or N-DG-dGal), or back to synthetic Man-rich (N-DG-Man).

Characterization of the glycosylated enzymes revealed an average incorporation of 10–15 carbohydrates per enzyme molecule: N-WT→N-WT-Gal (+14 Gal); N-DG→N-DG-Gal (+11); N-DG→N-DG-dGal (+10); N-DG→N-DG-Man (+15 Man) as determined by matrix-assisted laser desorption ionization MS . Enzyme activity, as judged by full Michaelis–Menten kinetic analysis, was enhanced or undisturbed by glycosylation and, even after high levels of glycosylation, the k_{cat}/K_M values of all the synthetically glycosylated enzymes were greater than or equal to the k_{cat}/K_M values of N-DG and in some cases were >200% enhanced (e.g., N-DG-dGal 72.5 $s^{-1}\cdot M^{-1}$ and N-DG 19.5 $s^{-1}\cdot M^{-1}$). Therefore, all these glycosylated enzymes displayed activities sufficiently high for use in LEAPT.

***In Vivo* Targeting Efficacy.** The ability of these glycosylated enzymes to be selectively localized *in vivo* while retaining the activity required to activate prodrug was established by using three methodologies: (*i*) gamma scintigraphy of radiolabeled glycosylated enzymes to determine organ localization (Fig. 2); (*ii*) microautoradiography of radiolabeled glycosylated enzymes to determine cell-type localization (Fig. 3A and B); and (*iii*) confocal microscopy and HPLC analysis of targeted release of the prodrug to the active drug by targeted glycosylated enzymes (Fig. 3C).

Gamma Scintigraphic Determination of *in Vivo* Organ Distribution. Gamma scintigraphy allowed quantitative, noninvasive assessment of *in vivo* distribution (31). In particular, the intensity of scintillation provided by ^{123}I labeling allowed good precision in biodistribution analysis. In addition to basic distribution analysis, competing blocking agents such as AF were used to dissect the underlying mechanism of biodistribution and organ uptake (Fig. 2A and supporting information). AF is a known ligand for the ASGPR (13), which serves to remove the ASGPR from cell surfaces by initiating RME. Such uptake competition experiments allowed a greatly reduced animal group in comparison with standard time course dissection techniques.

The natural Man-rich "high-mannose" glycosylation pattern (24) and corresponding *in vivo* distribution of ^{123}I-labeled N-WT acted as a benchmark for other glycosylated enzymes; 29% of the dose localized within the liver within 10 min by virtue of these existing carbohydrates. To investigate the role of carbohydrates in the uptake of N-WT, the wild-type enzyme was deglycosylated with endo-H to form N-DG, and a corresponding reduction in liver localization was observed. The role of Man in liver localization was further determined by investigating the difference in liver localization between N-DG and N-DG-Man. Man-specific receptors for macromolecules are known to play an important role in glycoprotein distribution (14), and a smaller (28%) increase in liver localization was observed for N-DG-Man, compared with N-DG-Gal (see below).

The engineered Gal-induced, carbohydrate-mediated uptake was investigated by determining the level of liver localization of glycosylated N-WT-Gal and N-DG-Gal, with (+AF) and without (−AF) selective blocking of the ASGPR receptor. We were pleased to discover that galactosylation (N-DG→N-DG-Gal) resulted in 31% of the N-DG-Gal dose being delivered to the liver, which was reduced to 9% when the ASGPR was challenged with AF (+AF); we conclude that this baseline level of uptake is due to noncarbohydrate-mediated uptake into nonparenchymal cells (31). (The possibility that some uptake may also be mediated by the GlcNAc residues that are left after endo-H-mediated deglycosylation cannot be discounted.) Thus, the glycosylation-engineering process shown in Fig. 1B allowed a complete retuning of the overall protein glycosylation pattern (N-WT→N-DG-Gal represents a transformation from native Man-rich high-mannose to Gal-rich), and it generated an 81% increase in liver localization (N-DG→N-DG-Gal).
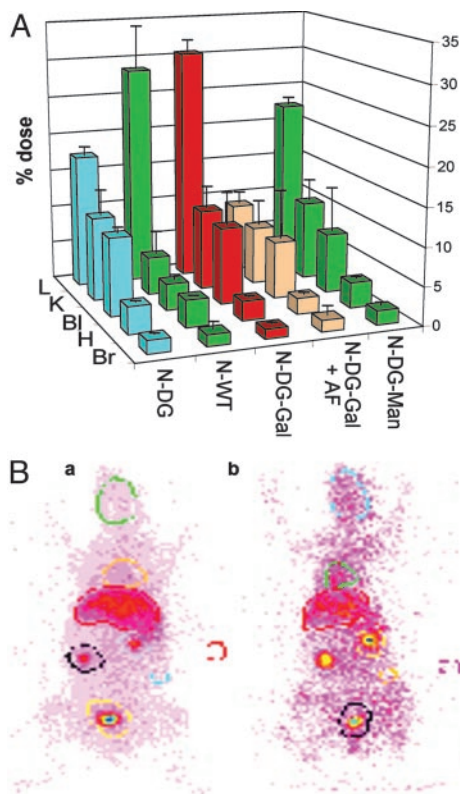
Fig. 2. Gamma scintigraphic determination of *in vivo* organ distribution. (*A*) The *in vivo* distribution of ^{123}I-labeled enzymes was determined. Male New Zealand White rabbits (*n* = 3–4; error bars show standard deviation) were dosed with enzyme (2.5 mg/kg) and, where appropriate, predosed with blocker (AF, 100 mg/kg). Images were recorded to investigate organ uptake selectivity and corresponding blood samples were taken at regular intervals. Key regions of interest were investigated (L, liver; K, kidney; Bl, bladder; H, heart/lungs; Br, brain) and normalized against background *in vivo* levels. Here levels at *t* = 10 min are shown. In all cases, postmortem organ analysis confirmed the values obtained by gamma scintigraphy image analysis. Gal-rich enzymes are shown in red and peach, Gal-Man mix enzymes are shown in yellow, and Man-rich are in green. N-DG-Gal displays sugar-dependent liver uptake that is most strongly blocked by AF (see main text). See supporting information for data for all constructs. (*B*) Representative images. Male New Zealand White rabbits dosed with ^{123}I-labeled N-DG-Gal, without (*Ba*) and with (*Bb*) predose of AF (N-DG-Gal + AF). Strong localization within the liver is observed when the ASGPR is not blocked compared with when AF is dosed, which results in higher levels of circulating N-DG-Gal. Selected organ regions are highlighted. Male New Zealand White rabbits were used in this study for their enhanced organ definition in imaging. Qualitatively similar data were obtained from male Wistar rats (see supporting information).

Time Course of Biodistribution. Taken together, blood samples obtained at regular intervals and gamma scintigraphic results highlighted a rapid serum clearance of glycosylated enzyme (see supporting information). After only 10 min <3% of the N-DG-Gal dose is in circulation. In contrast, when blocked by AF competition, 25% of the dose remains in circulation and, even after 2 h, 8% of N-DG-Gal is blocked and still circulates. The time course for hepatocyte uptake of N-DG-Gal ± AF also illustrates the clear difference in uptake attributable to the ASGPR: rapid uptake occurs for N-DG-Gal − AF (within 10 min) of the enzyme dose. With ASGPR blocking (N-DG-Gal + AF) uptake is ≈3.5-fold slower (N-DG-Gal, $t_{1/2} \approx 2$ min, 97% serum clearance after 10 min; N-DG-Gal + AF, $t_{1/2} \approx 7$ min, 69% serum clearance after 10 min).

Microautoradiographic Determination of *in Vivo* Cellular Targeting Efficacy. The cell-type-specific localization of glycosylated enzymes within the liver was investigated by using microautoradiography
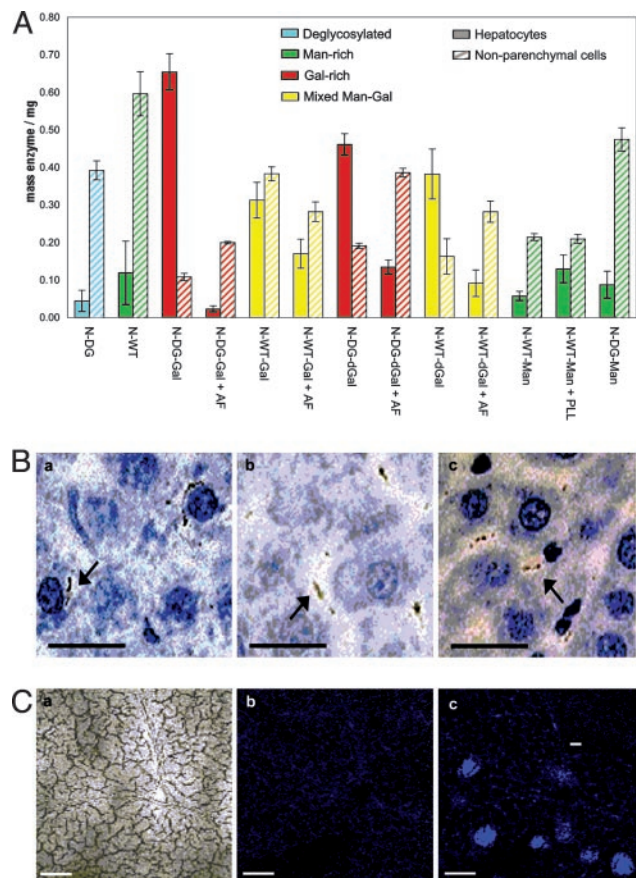

Fig. 3. Cellular localization. (*A*) Microautoradiographic determination of *in vivo* cellular localization. The *in vivo* cell-type localization of ^{3}H-labeled enzymes within the liver was determined by microautoradiography in combination with organ distribution data. Sugar-dependent trends emerge. There is a dramatic switch in cell localization from Man-rich N-WT [lane 2, localized predominantly in nonparenchymal cells (hatched bars)] to Gal-rich N-DG-Gal [lane 3, localized predominantly in hepatocytes (filled bars)], which have similar gross organ uptake levels but contrasting cell destinations. (*B*) Representative microautoradiography images. Liver samples from male Wistar rats dosed with ^{3}H-labeled enzymes. Hepatic nuclei are clearly stained dark blue, associated cytoplasm is stained light blue, and sinusoidal regions are pale blue/white. Dark black regions indicate presence of ^{3}H-labeled glycosylated enzyme. N-DG-Gal (*Ba*) localizes predominantly in hepatocyte cytoplasm. In contrast, the predose of AF (N-DG-Gal + AF; *Bb*) or lack of galactosylation (N-DG; *Bc*) prevents hepatocyte uptake by the ASGPR and leads to localization in predominantly nonparenchymal cell regions. (Scale bar, 25 μm.) (*C*) Confocal microscopy. (*Ca*) Phase image illustrates the architecture of a liver section from an N-DG-Gal-dosed male Wistar rat; plates of hepatocytes surround a central blood vessel. (*Cb*) Fluorescence image of the same section without MEND-Rha (some collagen-derived autofluorescence is observed). (*Cc*) Fluorescence image of the same section with prodrug MEND-Rha. Strong fluorescence demonstrates release of MEND in the hepatocyte region. (*Inset*) Fluorescence image from undosed animal with MEND-Rha. (Scale bar, 0.1 mm.)

(32) (Fig. 3). Coupled with the organ distribution data above, this allowed the determination of the total mass of enzyme delivered specifically to the hepatocytes (parenchymal) and nonparenchymal cells (Fig. 3*A*). N-WT displayed an increased total level of liver localization over N-DG but similar ratios of hepatocyte to nonparenchymal cell localization. This finding indicates that N-DG undergoes non-carbohydrate-specific uptake predominantly into nonparenchymal cells. This nonparenchymal uptake is enhanced in Man-rich N-WT by the native high-mannose glycosylation, which results in carbohydrate-specific uptake by mannose receptors into nonparenchymal cells.

The chemical galactosylation of N-DG to form Gal-rich N-DG-Gal restored a total level of liver localization similar to that for N-WT. However, in striking contrast to both N-DG and N-WT, 86% of the N-DG-Gal dose was located within the hepatocytes of the liver. This dramatic reversal (Fig. 3A) from 90% nonparenchymal selectivity in N-DG to 86% hepatocyte selectivity in N-DG-Gal represents an overall switch in selectivity of 60-fold and provides clear evidence for the modulation by glycosylation of uptake of these glycosylated enzymes. Similarly, the complete alteration of glycosylation from Man-rich to Gal-rich, N-WT→N-DG→N-DG-Gal, also resulted in a dramatic nonparenchymal cell to hepatocyte switching.

This glycosylation-retuning method was also used to switch the natural Man-rich high-mannose-type glycosylation to synthetic Man-rich glycosylation, N-WT → N-DG → N-DG-Man. The fidelity of the glycosylation method was shown by the abolition and then regeneration of biodistribution consistent with mannosylation, N-WT(Man-rich)→N-DG(Man-poor)→N-DG-Man(Man-rich). This further highlighted the useful modular nature of this glycosylation retuning in its ability to generate Gal-like or Man-like properties through the appropriate choice of protein glycosylating reagent.

The role of the ASGPR in this highly specific cellular localization of N-DG-Gal was determined by contrasting the values for N-DG-Gal with and without predosed AF blocker (±AF). In addition to the overall localization to the liver being greatly reduced on blocking of the ASGPR by AF, it is evident that this reduction is due to a near abolition of hepatocyte uptake from 0.66 to 0.02 mg. When uptake of N-DG-Gal was blocked by AF, an accompanying increase also occurred in uptake into nonparenchymal cells, possibly because of enhanced non-carbohydrate-specific uptake, promoted by an increased concentration of N-DG-Gal in the serum.

The glycosylated enzymes displaying branched, multivalent arrays of carbohydrates, N-DG-dGal and N-WT-dGal, also showed enhanced levels and selectivity of uptake as compared with N-DG (hepatocyte uptake of 0.04 mg of N-DG → 0.39 mg of N-WT-dGal and 0.47 mg of N-DG-dGal). Furthermore, enhancement in hepatocyte uptake (from 0.32 to 0.39 mg) and selectivity (2.9-fold) was observed for branched, multivalent N-WT-dGal over multiple monovalent N-WT-Gal. This trend did not extend to N-DG-dGal, and the multivalent display of similar levels of glycosylation (≈10 Gal) in N-DG-dGal as compared with monovalent N-DG-Gal appears to have reduced the ability of the ASGPR to selectively endocytose that enzyme. It may be that, in the case of N-DG-dGal, more crowded display of the same number of Gal carbohydrates is less suitable (33) or, on the other hand, yet higher levels of branching may be required to observe a greater multivalent effect.

From the foregoing biodistribution data, clear sugar-dependent trends emerge (Fig. 3B): (i) Man-rich or DG enzymes (N-DG, N-WT, N-WT-Man, and N-DG-Man) localize in nonparenchymal cells; (ii) Gal-rich enzymes (N-DG-Gal and N-DG-dGal) localize primarily in hepatocytes, a localization that is blocked by AF; and (iii) mixed Man-Gal-glycosylated enzymes (e.g., N-WT-Gal) show reduced localization preference. Thus, different glycosylation patterns determine localization patterns.

Targeted Prodrug Activation to Active Drug by Glycosylated Enzyme. After this cell-selective localization, the ability of the delivered, glycosylated α-L-rhamnosidase enzyme to selectively cleave a Rha-capped prodrug to release an active drug molecule to complete the LEAPT strategy was demonstrated. It has been shown that the ASGPR successfully internalizes Rha-displaying glycoconjugates.[‡‡] We used MEND, a fluorescent, coumaric, choleretic agent (34), as

[‡‡]Lerchen, H.-G., Baumgarten, J., von dem Bruch, K., Sperzel, M., Clemens, G. R. & Firbig H.-H., 2nd European Community Conference of Carbohydrate Drug Research (ECCDR2), September 14–17, 2000, Lisbon, Portugal, abstr. PL8.

a representative liver drug that is also a fluorophore, thereby allowing ready detection. MEND was conjugated to Rha by its 7-hydroxyl group to form MEND-Rha, as a Rha-capped prodrug for the LEAPT system. Capping of the 7-hydroxyl group in MEND removes its activity as a drug (35). Cleavage of the α-L-rhamnosidic bond by the delivered LEAPT enzyme α-L-rhamnosidase regenerates the parent drug MEND.

After application, the release of MEND from MEND-Rha by hepatocyte regions of the liver containing targeted rhamnosidase N-DG-Gal was clearly observed (Fig. 3Cc) by confocal microscopy. The lack of fluorescence on treatment of an undosed liver section with MEND-Rha illustrates the lack of α-rhamnosidase activity in normal hepatocytes (Fig. 3Cc Inset) and therefore the high specificity of drug release; active drug can only be released in the presence of prelocalized glycosylated rhamnosidase enzyme. This targeted drug release was also supported by HPLC analysis of relative levels of the released, active drug MEND in livers of dosed animals and absence in untreated animals (2.38 mg/kg MEND released in dosed livers 10 min after MEND-Rha treatment, compare with no detectable MEND in the undosed).

Furthermore, observed high levels of rhamnosidase activity present only in treated livers and completely absent in untreated livers were also further supported by enzyme activity assays of liver homogenate (see supporting information). As a consequence of this targeted delivery, enzyme activity levels in the liver and in the serum in treated animals differ greatly. Calculations suggest that the enzyme levels present after 10 min would create through targeting a typical serum/hepatocyte drug concentration ratio of ≈1:590 (see supporting information).

Glycosylated Enzyme Stability. LEAPT achieves enhanced selectivity of drug release by exploiting RME to internalize the delivered glycosylated enzyme within specific cells. RME mechanisms employ intracellular trafficking pathways that form endosomes around internalized ligands (12). An important parameter in this strategy, therefore, is the stability of the delivered enzyme toward possible degradation within intracellular compartments. The level of rhamnosidase activity conferred by N-DG-Gal on delivery to the liver was higher than that created by a comparable mass of other glycosylated enzymes (see supporting information). Thus, 0.76 mg of N-DG-Gal delivered with 83% hepatocyte selectivity created >5 times the enzyme activity (0.20 unit) of 0.72 mg of N-WT with 90% nonhepatocyte selectivity (0.04 unit). The origin of this higher activity was probed with representative lysosomal enzyme preparations from rat liver (36). Chemical glycosylation of N-DG→N-DG-Gal substantially enhanced the stability of N-DG, extending its half-life under these conditions from 1 h for N-DG to >48 h for N-DG-Gal. This powerful stabilizing effect is consistent with previous observations that glycans on proteins enhance the stability of glycoproteins toward proteolytic degradation (37). Treatment with trypsin revealed that part but not all of the enhanced stability of N-DG-Gal is due to greater resistance to tryptic degradation created by the chemical glycosylation of the lysine side chains that are recognized by trypsin.

***In Vivo* Therapeutic Efficacy.** Finally, to establish the therapeutic effectiveness of the LEAPT strategy, a preliminary disease model study was conducted. After intrasplenic injection of the human hepatocellular liver carcinoma cell line HepG2 into nude (*nu/nu*) athymic mice, three trial groups (*n* = 13) were treated with the complete LEAPT system (prodrug plus enzyme) or dosed with the individual components alone (enzyme or prodrug, respectively) as controls. To treat this tumor disease model the well studied cytotoxic DOX (38) was selected as a representative drug and the Rha-capped, DOX-conjugate prodrug DOX-Rha was synthesized for use in the LEAPT system. The LEAPT system therefore consisted of N-DG-Gal administration (2.5 mg/kg) followed, after sufficient time for liver targeting (20 min), by dosing of prodrug

Table 1. *In vivo* efficacy of LEAPT in liver tumor disease model

	Control		Treated
	N-DG-Gal alone	DOX-Rha alone	N-DG-Gal + DOX-Rha
Total tumor foci	17 ± 0.5	23 ± 4.4	11 ± 0.7
Total tumor burden	570 ± 18.5	690 ± 130	390 ± 25.0

Total liver tumor burden and foci in the treated group (*n* = 13), 42 days of three-times-weekly dosing with the complete LEAPT [N-DG-Gal (2.5 mg/kg) + DOX-Rha (10 mg/kg)] system, are significantly reduced as compared with the control groups (both *n* = 13) of enzyme (N-DG-Gal) alone and prodrug (DOX-Rha) alone.

DOX-Rha (10 mg/kg). After 42 days of three-times-weekly dosing, the liver tumor burden was histologically quantified (Table 1) and revealed, even in this unoptimized dosing regime, a near halving in total tumor burden (from 690 to 370) and a slightly greater than halving of total tumor foci in the treated group as compared with the control group of unactivated prodrug alone (from 23 to 11). Consistent with the need for coadministration of both components for the LEAPT strategy to be effective, no significant difference was seen between the two control groups of capped, unactivated prodrug alone and enzyme without drug alone.

Conclusion

We have discovered that it is possible to exploit an endogenous, carbohydrate–protein binding process to internalize enzymes within predetermined cell types and to use the enzyme activity that is localized to activate prodrugs *in situ*. This activation in turn benefits the desired outcome of higher concentrations of active drug for localized drug delivery at a target site.

The system achieves these higher concentrations of active drug through the use of precisely glycosylated enzymes. Because, in the liver-targeted systems studied here, the uptake mechanism is specific to the carbohydrate used and the glycosylation pattern on the enzyme can be simply altered, it was possible to readily redirect the enzyme to another cell type without the need for extensive generation of another (e.g., antibody) binding system. *In vivo* experiments demonstrated that such retooling using Gal generates a dramatic reversal in cell selectivity from 90% localization in nonhepatocytes before correct glycosylation to 86% localization in hepatocytes after Gal-rich glycosylation. This reversal allowed a >30-fold enhancement in the absolute level of enzyme delivered to hepatocytes (from 0.02 to 0.66 mg) and created exogenous enzyme activities (for N-DG-Gal, 0.20 unit of enzyme activity delivered to hepatocytes) that we believe are the highest yet demonstrated through such delivery. Confocal microscopy showed highly localized prodrug activation by this enzyme activity and zero activation in the absence of enzyme. Furthermore, glycosylation enhanced the rate of uptake of the protein component from serum, thereby reducing the time for potential immunogenic exposure, and substantially enhanced the enzyme's stability under degradative conditions that represent those found *in vivo*. Initial promising data from the treatment of a preliminary tumor disease model suggests that together these beneficial indications create therapeutic effectiveness in the LEAPT system.

Because some other endogenous carbohydrate-binding processes exist that are similar to that exploited here (13, 14, 39), we suggest that the LEAPT system may be applicable to other cell types, with the possibility of specific carbohydrates allowing specific cell targeting. The applicability of such an approach will depend on the identification of suitable receptors of potential medical relevance, e.g., the use of macrophage-associated carbohydrate receptors (14, 39) to treat macrophage-associated diseases such as lysosomal storage disease (40) or viral infections (41). Moreover, the additional benefit of rhamnose targeting (and hence double targeting) in the current liver LEAPT system might be lost in other tissue/cell systems, necessitating a reliance on passive small-molecule mechanisms such as pinocytosis. The ability to target hepatocytes shown here might be of benefit, for example, in the treatment of hepatocyte-associated diseases such as hepatocarcinomas, as shown here in a preliminary HepG2-mouse disease model, or in others, such as hepatitis. To this end, we focus on the delivery of cytotoxic and antiviral compounds by using LEAPT. [Animal experiments were licensed by U.K. Home Office (Licenses PPL 40/1642, PPL 80/01197, PPL 40/1387, and PPL 40/2323) and subject to the U.K. Animals (Scientific Procedures) Act 1986.]

1. Varki, A. (1993) *Glycobiology* **3**, 97–130.
2. Weis, W. I. & Drickamer, K. (1996) *Annu. Rev. Biochem.* **65**, 441–473.
3. Dwek, R. A. (1996) *Chem. Rev.* **96**, 683–720.
4. Seto, N. O. L. & Evans, S. V. (2000) *Curr. Org. Chem.* **4**, 411–427.
5. Yamazaki, N., Kojima, S., Bovin, N. V., Andre, S., Gabius, S. & Gabius, H.-J. (2000) *Adv. Drug Delivery Rev.* **43**, 225–244.
6. Davis, B. G. & Robinson, M. A. (2002) *Curr. Opin. Drug Discov. Dev.* **5**, 279–288.
7. Gabius, S., Kayser, K., Bovin, N. V., Yamazaki, N., Kojima, S., Kaltner, H. & Gabius, H.-J. (1996) *Eur. J. Pharm. Biopharm.* **42**, 250–261.
8. Beljaars, L., Melgert, B. N., Meijer, D. K. F., Molema, G. & Poelstra, K. (2001) in *Drug Targeting Technology*, ed. Schreier, H. (Dekker, New York), Vol. 2, pp. 183–210.
9. Bagshawe, K. D. (1994) *J. Controlled Release* **28**, 187–193.
10. Wentworth, P., Datta, A., Blakey, D., Boyle, T., Partridge, L. J. & Blackburn, G. M. (1996) *Proc. Natl. Acad. Sci. USA* **93**, 799–803.
11. Fonseca, M. J., Storm, G., Hennink, W. E., Gerritsen, W. R. & Haisma, H. J. (1999) *J. Gene Med.* **1**, 407–414.
12. Vyas, S. P., Singh, A. & Sihorkar, V. (2001) *Crit. Rev. Ther. Drug Carrier Syst.* **18**, 1–76.
13. Ashwell, G. & Morell, A. G. (1974) *Adv. Enzymol. Relat. Areas Mol. Biol.* **41**, 99–128.
14. Lee, S. J., Evers, S., Roeder, D., Parlow, A. F., Risteli, J., Risteli, L., Lee, Y. C., Feizi, T., Langen, H. & Nussenzweig, M. C. (2002) *Science* **295**, 1898–1901.
15. Lis, H. & Sharon, N. (1998) *Chem. Rev.* **98**, 637–674.
16. Duncan, R., Kopeček, J., Rejmanova, P. & Lloyd, J. B. (1983) *Biochim. Biophys. Acta* **755**, 518–521.
17. Fujita, T., Nishikawa, M., Tamaki, C., Takakura, Y., Hashida, M. & Sezaki, H. (1992) *J. Pharmacol. Exp. Ther.* **263**, 971–978.
18. Nishikawa, M., Tamada, A., Kumai, H., Yamashita, F. & Hashida, M. (2002) *Int. J. Cancer* **99**, 474–479.
19. Friedman, B. A., Vaddi, K., Preston, C., Mahon, E., Cataldo, J. R. & McPherson, J. M. (1999) *Blood* **93**, 2807–2816.
20. Lee, Y. C., Stowell, C. P. & Krantz, M. J. (1976) *Biochemistry* **15**, 3956–3963.
21. Stowell, C. P. & Lee, Y. C. (1982) *Methods Enzymol.* **83**, 278–288.
22. Laboratory Animal Science Association (1998) *Good Practice Guidelines: Collection of Blood Samples* (Laboratory Animal Science Association, Tamworth, U.K.).
23. Fraker, P. J. & Speck, J. C. (1978) *Biochem. Biophys. Res. Commun.* **80**, 849–857.
24. Young, N. M., Johnston, R. A. Z. & Richards, J. C. (1989) *Carbohydr. Res.* **191**, 53–62.
25. Tarentino, A. L. & Trimble, R. B. & Maley, F. (1978) *Methods Enzymol.* **50**, 574–580.
26. Mort, A. J. & Lamport, D. T. A. (1979) *Anal. Biochem.* **81**, 289–309.
27. Staud, F., Nishikawa, M., Takakura, Y. & Hashida, M. (1999) *Biochim. Biophys. Acta* **1427**, 183–192.
28. Lee, Y. C., Townsend, R. R., Hardy, M. R., Lönngren, J., Arnarp, J., Haraldsson, M. & Lönn, H. (1983) *J. Biol. Chem.* **258**, 199–202.
29. Davis, B. G. (2002) *Chem. Rev.* **102**, 579–601.
30. Perkins, A. & Frier, M., eds. (2000) *Nuclear Medicine in Pharmaceutical Research* (Taylor & Francis, London)
31. Smedsrød, B., Debleser, P. J., Braet, F., Lovisetti, P., Vanderkerken, K., Wisse, E. & Geerts, A. (1994) *Gut* **35**, 1509–1516.
32. Baker, J. R. J. (1989) *Automicroradiography: A Comprehensive Overview*, Royal Microscopical Society Microscopy Handbook 18 (Oxford Scientific, Oxford).
33. Opanasopit, P., Shirashi, K., Nishikawa, M., Yamashita, F., Takakura, Y. & Hashida, M. (2001) *Am. J. Physiol.* **280**, G879–G889.
34. Swiss Pharmaceutical Society (2000) *Index Nominum 2000: International Drug Directory* (Medpharm GmbH Scientific Publishers, Stuttgart, Germany)
35. Everett, S. A., Swann, E., Naylor, M. A., Stratford, M. R. L., Patel, K. B., Tian, N., Newman, R. G., Vojnovic, B., Moody, C. J. & Wardman, P. (2002) *Biochem. Pharmacol.* **63**, 1629–1639.
36. Trouet, A. (1974) *Methods Enzymol.* **31**, 323–329.
37. Rudd, P. M., Joao, H. C., Coghill, E., Fiten, P., Saunders, M. R., Opdenakker, G. & Dwek, R. A. (1994) *Biochemistry* **33**, 17–22.
38. Launchbury, A. P. & Habboubi, N. (1993) *Cancer Treat. Rev.* **19**, 197–228.
39. Brown, G. D. & Gordon, S. (2001) *Nature* **413**, 36–37.
40. Beutler, E. (1988) *Blood Rev.* **2**, 59–70.
41. Aquaro, S., Bagnarelli, P., Guenci, T., De Luca, A., Clementi, M., Balestra, E., Calio, R. & Perno, C. F. (2002) *J. Med. Virol.* **68**, 479–488.